Contrib Mineral Petrol (1998) 131: 364–378

Stuart Black · Ray Macdonald · Barbara A. Barreiro
Peter N. Dunkley · Martin Smith

Open system alkaline magmatism in northern Kenya: evidence from U-series disequilibria and radiogenic isotopes

Received: 29 May 1996 / Accepted: 24 November 1997

Abstract U-series activity ratios, Sr-Nd-Pb isotopic ratios and major and trace element compositions have been determined on young basalts (<10 ka) and trachytes from the volcano Emuruangogolak in the Kenya Rift Valley. The basalts are mildly alkaline and are associated with small volumes of hawaiite. The mafic rocks are characterised by high ($^{230}Th/^{232}Th$) (≥ 1.06) with low ($^{238}U/^{230}Th$) ratios (≤ 0.72). They have variable incompatible trace element ratios (e.g. Zr/Nb, Ba/Zr), indicating that they represent a number of magmatic lineages. The trachytes, which comprise both comenditic and pantelleritic varieties, have significantly lower ($^{230}Th/^{232}Th$) ratios than the basalts, with clear differences between pantelleritic and comenditic types. The ($^{238}U/^{230}Th$) ratios in the pantellerites range from less, to greater, than 1. The variations in composition and isotopic diversity must represent different sources for the trachytes. Internal isochrons for the trachytes give U-Th ages of 14 to 40 ka, similar to single crystal laser fusion $^{40}Ar/^{39}Ar$ ages from sanidine phenocrysts (16–38 ka) for the same rocks. Post-crystallisation residence times of the trachytes were very short, implying relatively rapid movement of trachyte from magma chamber to the surface. Variations in the initial $(^{230}Th/^{232}Th)_0$ ratios (0.69–1.14) of both basalts and trachytes indicate that Emuruangogolak has erupted a large range of isotopically diverse magmas over a very short period of time (38 ka), from conduits closely spaced around the summit of the volcano.

S. Black[1] (✉) · R. Macdonald
Environmental Science Division,
IEBS, Lancaster University, Lancaster, LA1 4YQ, UK,
Tel.: 01524 594209; Fax: UK 01524 593985;
E-mail: s.black@lancaster.ac.uk

Present address:
[1]PRIS, University of Reading, Whiteknights,
Reading RG6 6AB, UK
Tel.: 0118 931 6713; Fax: UK 0118 931 0279
E-mail: s.black@reading.ac.uk

B.A. Barreiro
NERC Isotope Geoscience Laboratory, Keyworth,
Nottingham, NG12 5GG, UK

P.N. Dunkley
British Geological Survey, Keyworth, Nottingham,
NG12 5GG, UK

M. Smith
British Geological Survey, Murchison House,
West Mains Road, Edinburgh, EH9 3LA, UK

Editorial responsibility: I. Parsons

Introduction

The nature and efficiency of differentiation processes in crustal magma chambers are dependent, *inter alia*, on magma residence times, which are poorly constrained for most volcanic systems. The U-series disequilibria systematics have been used in two studies of residence times in basalt-trachyte/phonolite centres. Widom et al. (1992) found, for rocks of San Miguel in the Azores, that the time from formation of a parental alkali basalt by partial melting of mantle to generation and eruption of the Fogo trachytes was rather less than 10^5 years, and that zoned trachytic cupolas have developed in <4600 years. Broadly similar timescales may have characterized the evolution of the basanite-phonolite Laacher See volcano in Germany. Differentiation of parental basanite to mafic phonolite took some 10^5 years. Further evolution of the phonolitic magmas in high-level chambers took some $1–2 \times 10^4$ years (Bourdon et al. 1994).

Here we use two approaches to understanding the nature of the magmatic plumbing system beneath the Emuruangogolak basalt-trachyte complex in northern Kenya, and to quantifying the timescales of magmatic evolution. Firstly, major and trace element and isotopic data are used to show that, in the last 38 ka at least, Emuruangogolak has been a very open system, with essentially coeval eruption of genetically unrelated magmas. Secondly, U-series disequilibria data are employed to determine residence times of trachyte magmas within crustal reservoirs and to support the case for the open system nature of basalt-trachyte magma production.

Geology

The major Quaternary caldera volcanoes of the inner trough of the Kenya rift valley fall into two sets (Williams et al. 1984; Macdonald 1987). The *northern* set (the Barrier Volcanic Complex, Emuruangogolak, Silali, Paka and Korosi) are dominantly trachytic, and basalt is volumetrically more abundant than rocks of mugearitic or trachybasaltic composition. The *southern* set (Menengai, Longonot and Suswa) are almost entirely trachytic, although eruption of basalt as components of mixed magmas at Longonot suggests that basalt magma has been involved in the volcanic systems. Magmas of intermediate composition have been recorded only at Suswa, where they are represented by volumetrically minor, syn-caldera, trachybasaltic pyroclastic deposits (Skilling 1993).

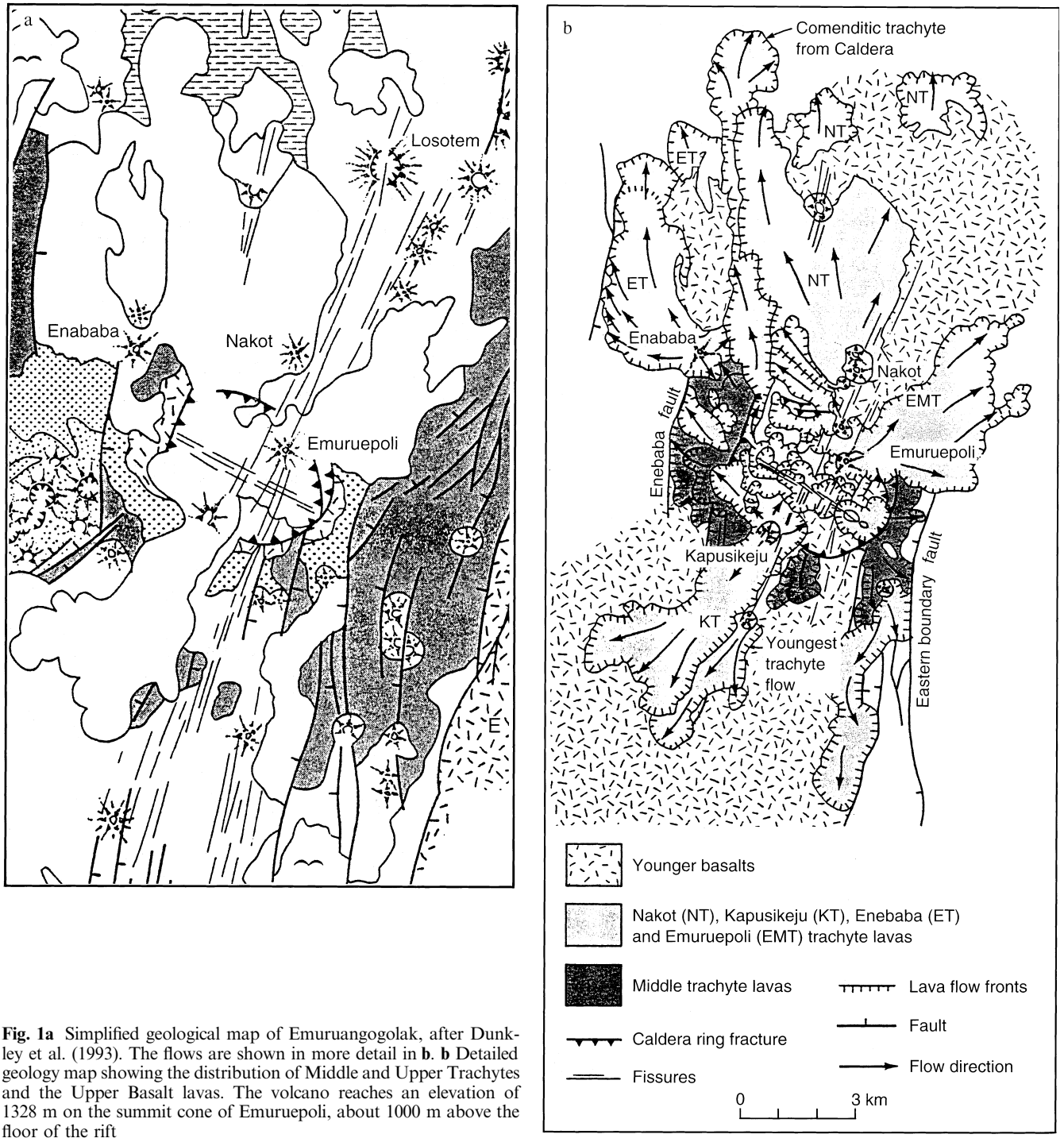

Fig. 1a Simplified geological map of Emuruangogolak, after Dunkley et al. (1993). The flows are shown in more detail in **b**. **b** Detailed geology map showing the distribution of Middle and Upper Trachytes and the Upper Basalt lavas. The volcano reaches an elevation of 1328 m on the summit cone of Emuruepoli, about 1000 m above the floor of the rift

The major Quaternary volcanic stratigraphy of Emuruangogolak is summarised in Figs. 1a,b and 2 (Dunkley et al. 1993). The centre comprises a large shield volcano with a summit caldera. It is composed of silica-oversaturated, peralkaline trachyte lavas and pyroclastic rocks, together with weakly undersaturated basalts, the proportion of trachyte to basalt being approximately 10:1.

In an earlier phase of activity (>900–500 ka), a shield of similar extent and height to the present day volcano was formed by eruption of the Lower Trachyte Lavas (Fig. 2). The N–S faulting of the early shield was then apparently followed by a long period of quiescence between 500 and 205 ka.

At around 205 ka, the trachytic Lower Pyroclastic Deposits were erupted from a series of pumice cones located on N- to NNE-trending fractures on the upper western flanks (Fig. 1a). These were closely followed by the effusion of uniformly thin, Lower Basaltic Lavas (185 ± 11 ka) from fissures high on the western flanks. A return to trachytic magmatism resulted in eruption of the undated Middle Trachyte Lavas from a number of vents on the summit area and uppermost flanks. The 38 ± 6 ka Upper Pyroclastic Deposits (Fig. 2) overlie the Middle Trachytes and were erupted from pyroclastic cones on the uppermost flanks. Collapse of the summit area to form a caldera followed shortly afterwards (Dunkley et al. 1993).

The Upper Trachyte Lavas, erupted from NNE-trending fissures and faults located high on the volcano flanks and from NNE- and NW-trending fissure zones on the caldera floor, form a series of spectacular lava cones and domes. Ar-Ar dating indicates that the majority of the lavas post-date caldera formation; however, those from Enababa, dated at 38 ± 3 ka, suggest that activity overlapped with caldera formation. Dunkley et al. conclude that the caldera formed as a response to flank eruption of the earliest of the Upper Trachyte Lavas and associated explosive eruption of the Upper Pyroclastic Deposits across the summit area.

The final phase of activity on Emuruangogolak is represented by the Upper Basalt Lavas. These voluminous and largely pristine lavas overlap in age the Upper Trachyte Lavas (>38 ka to *c.* 1900 A.D.) and were erupted mainly from the northern and southern flanks of the volcano. In the north, lava interaction with the former Lake Suguta, along shorelines dated around 10 ka (Hillaire-Marcel et al. 1986), indicates activity mainly post-dating the Upper Trachytes. On the southern flanks, one basalt sample (KB46) dated at 250 ± 100 years (Dunkley et al. 1993) is overlain by a pristine trachyte flow estimated to have erupted at *c.* 1900 A.D. Several other basalt flows (KB145 and KB82) were dated to 700–900 B.P. by magnetic variation studies (Skinner et al. 1975). Other ages of 3–8000 years B.P. and >38,000 years B.P. have been reported on stratigraphic grounds (Dunkley et al. 1993).

Important features of the geological evolution of Emuruangogolak include the following:

1. Although no basaltic lavas were erupted during the earliest activity (Lower Trachyte Lavas), the presence of mixed basalt-trachyte flows in the group (Dunkley et al. 1993, p. 64) suggests that basaltic magma was present in the plumbing system at that time. Thus, basalt and trachyte magmas have been present during the whole evolution of the centre, sometimes being erupted essentially simultaneously (Fig. 2).
2. The combination of open, tensile fractures and linear trains of basaltic fissures and scoria cones, along with landforms typical of basaltic fissure eruption, is characteristic of crustal dilation in response to dyke injection. Dunkley et al. (1993) and Smith et al. (1995) envisage zones of multiple dyke injection emplaced very close to the surface beneath the northern centres. Gravity data for Silali and Emuruangogolak (Swain 1976) indicate the presence of narrow, linear,

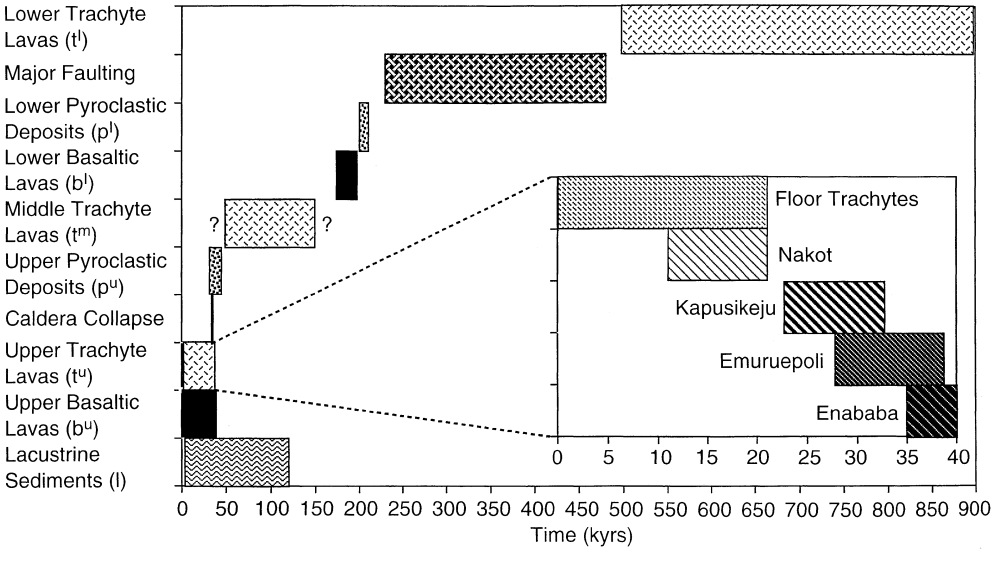

Fig. 2 Generalised sequence of the evolution of Emuruangogolak, after Dunkley et al. (1993). It should be noted that during the recent development of the volcano the Upper Trachytes and Upper Basalts were erupted during the same broad period

positive anomalies extending towards the south. These anomalies coincide with the zone of fracturing (NNE–SSW at 018°) and may reflect the presence of an axial dyke swarm intruded into the Precambrian basement at depths of 2–3 km. Modelling of the gravity data suggests dense basaltic bodies, approximately 11 km by 6 km, intruded to within 2 km of the surface (Swain 1992).

3. The Upper Trachytes contain two varieties; pantelleritic trachytes [mol $(Na_2O + K_2O)/Al_2O_3 = 1.16–1.57$] and comenditic trachytes (1.00–1.22). All are weakly silica oversaturated (normative quartz 0.84–3.5%). Rocks from Enababa, Nakot, Emuruepoli and Kapusikeju are pantelleritic, the remaining rocks from Kapusikeju and young flows on the northern and southern flanks are comenditic. Flows of both affinities have apparently been erupted from Kapusikeju.
4. Emuruangogolak is genuinely bimodal; no rocks of intermediate composition have been recorded, except as mixed magma products. This has been related at Emuruangogolak (Dunkley et al. 1993), and at the neighbouring volcano Silali (Macdonald et al. 1995), to two effects. Firstly, simple trace element modelling indicates that the transition between basalt and trachyte represents a small proportion (< 20%) of the total compositional range. Secondly, physical controls resulting from density and viscosity variations are also thought to have discriminated against the eruption of intermediate compositions.

Whilst the bulk of the basalts may have been erupted from dykes, the form of the reservoirs feeding the trachytes is uncertain. Dunkley et al. supposed that any high-level trachytic chamber has, or had, a diameter approximately the same as the associated caldera (5 km). The geographically and temporally close association of basalt and trachyte in post-caldera times makes it unlikely, however, that a substantial "shadow zone" (Mahood 1984) still underlies the centre, in that relatively dense basaltic magma should not be able to penetrate through a less dense trachytic reservoir. We must infer that the reservoirs feeding substantial trachytic activity on Emuruangogolak were transient, in order to allow subsequent basaltic dykes to penetrate them, an inference made by Macdonald et al. (1995) for Silali.

Samples and analytical procedures

For this study, we have chosen samples ranging from "historical" i.e. 250 ± 100 years, to prehistoric (700 years to 38 ka). Change in activity of ^{226}Ra in 100 years is < 1%, and during a period of 10–30 kyears, the age-related variation for ^{230}Th is still close to analytical error, however, all samples have been decay corrected to time of eruption. All but one of the 26 samples (a Lower Basalt) come from the Upper Basalts (5 samples) and Upper Trachytes (20 samples) and represent the most recent activity at Emuruangogolak. Divisions of the Upper Trachytes are given in Fig. 2; samples are allocated to divisions in Table 1a–c.

All the basalt samples are aphyric or glassy. Trachyte samples vary from microporphyritic to porphyritic varieties, with anorthoclase, sanidine, clinopyroxene and titanomagnetite phenocrysts with trace quantities of fayalite present. Major and trace element abundances in 31 samples (11 basalts/hawaiites and 20 trachytes) were analysed by XRF at the British Geological Survey, Keyworth and Lancaster University, using PHILIPS PW1400, PW1408 and PW1480 equipment, on fused tetraborate beads for major elements and pressed powder pellets for trace elements. Selected analyses are given in Table 1a–c; a full data set is available upon request from the corresponding author.

The Pb, Sr and Nd isotopes in a subset of 9 samples (Table 2) were analysed at the NERC Isotope Geoscience Laboratories. All three elements were extracted from the same dissolution of 100–150 mg of powdered rock sample in Savillex PFA Teflon jars. The Sr and Nd fractions were eluted in 2 ml 1N HBr, and the Pb eluted in 1 ml 6N HCl from anion exchange resin. The Sr and bulk REE (rare earth elements) were separated using conventional cation exchange techniques using HCl and Dowex 50 × 8, 200–400 mesh resin. The Nd was separated from the bulk REE on columns filled with Biobeads© coated with bis di-ethylhexyl hydrogen phosphate (HDEHP). Procedural blanks for Pb, Sr and Nd were less than 150 picogram, 1 nanogram and 400 picogram, respectively. The Sr and Pb isotopic compositions were measured in static mode on a Finnigan MAT 262 multicollector mass spectrometer on single Re filaments. The Nd was loaded onto Ta side filaments of a triple filament Ta-Re-Ta assembly, and Nd isotopic composition of the metal species was measured in dynamic mode on a VG 354 multicollector mass spectrometer. The $^{87}Sr/^{86}Sr$ was normalised to $^{86}Sr/^{88}Sr = 0.1194$, $^{143}Nd/^{144}Nd$ was normalised to $^{146}Nd/^{144}Nd = 0.7219$, and Pb isotope ratios are corrected for 1 per mil mass fraction per amu. Results for isotope standards during the three periods of measurements are: NBS 987 $^{86}Sr/^{88}Sr = 0.710236 \pm 0.000018$ ($n = 10$), 0.710235 ± 0.000017 ($n = 10$) and 0.710224 ± 0.000016 ($n = 10$), Johnson-Matthey Nd, $^{143}Nd/^{144}Nd = 0.511116 \pm 0.000010$ ($n = 10$), 0.511122 ± 0.000019 ($n = 10$) and 0.511111 ± 0.000010 ($n = 10$), La Jolla Nd, $^{143}Nd/^{144}Nd = 0.511853 \pm 0.000015$ ($n = 17$). All uncertainties are 1σ.

We have also determined U and Th concentrations and various U-series activity ratios on 20 samples, together with mineral separates from three of the trachytes from Emuruangogolak and one from the volcano Paka (Tables 3 and 4). The U-series radionuclides were measured by high resolution α-spectrometry at Lancaster University, after chemical separation and purification using conventional techniques (HF-HNO_3-HCl digestions, followed by anion exchange resin separation on 9 M HCl and 7.2 M HNO_3 columns, together with electrodeposition (Black 1994). Dissolutions of whole rock and mineral separates were performed on sample masses ranging from 0.5–2.0 and 0.8–5.1 grams, respectively. For U-Th analyses a ^{232}U-^{228}Th yield monitor was used with a decay and ingrowth correction applied for the daughter ^{224}Ra nuclide. Typical yields ranged from 70–100% for uranium and 80–100% for thorium. Blank and background determinations were carried out frequently averaging < 10 counts in 10,000 under determinant peaks and < 25 counts in 10,000 under the ^{232}U-^{228}Th yield monitor peaks. Whole rock samples were generally counted for between 2 and 6 days and mineral separates were counted for between 2 and 10 weeks.

For internal isochrons, separate phenocryst phases from single rock samples were used. Mineral and groundmass separates were made using standard magnetic and density techniques, followed by hand-picking to remove impurities (Black 1994; Black et al. 1997). Difficulty in obtaining absolutely pure separates was imposed by glass (melt) inclusions in the alkali feldspar, and microphenocrysts in groundmass separates. The estimated purity for feldspar and matrix was > 99.5%. The phases separated were groundmass, feldspar and a magnetic separate containing oxides, aegirine-augite, and fayalite. The ages were measured by the slope of the isochrons using a weighted regression method which takes into account the 2 s counting errors associated with each variable (Williamson 1968). The quality of the Lancaster U-Th data can be estimated

Tables 1a–c Major and trace element data for Emuruangogolak basalts and trachytes. (*Lw Bas* lower basalt, *Kapus* Kapusikeju, *Nak* Nakot, *Enab* Enababa, *Emur* Emuruopoli groups; *Floor** comendites erupted onto the floor of the rift from separate cones but not associated with any particular group). Major and trace elements analysed by XRF at British Geological Survey, Keyworth except KB244, KB245 and KB258 which were analysed at Lancaster University. U and Th were determined by α-spectrometry at Lancaster University

Table 1 a Major and trace element data for Emuruangogolak basalts and hawaiites (*ND* not determined, *LOI* loss on ignition)

Number	KB119	KB94	KB145	KB100	KB46	KB82	KB59	KB121
Centre	Kapus	Emur	Nak	- - - - -	Kapus	Kapus	Enab	Lw Bas
Composition	B	B	B	B	H	H	H	H
(Wt%)								
SiO_2	47.67	46.22	45.74	45.94	46.30	46.12	46.06	48.73
TiO_2	1.84	2.74	3.85	3.85	3.83	3.81	1.59	3.58
Al_2O_3	15.66	14.78	13.77	13.69	13.87	13.97	20.86	13.57
Fe_2O_3	10.58	13.61	15.59	15.38	15.35	15.37	9.15	14.08
MnO	0.15	0.19	0.24	0.22	0.25	0.23	0.13	0.25
MgO	7.42	6.68	5.27	5.15	4.83	4.80	4.03	4.07
CaO	11.87	11.36	10.15	9.90	9.45	9.47	12.52	8.19
Na_2O	2.91	3.14	3.48	3.93	4.03	4.14	3.33	4.48
K_2O	0.96	0.80	1.10	1.10	1.26	1.22	0.41	1.55
P_2O_5	0.41	0.58	0.99	1.18	1.12	1.15	0.24	1.77
LOI	0.55	0.00	0.88	0.00	0.00	0.00	1.69	0.00
Total	100.02	100.10	101.06	100.34	100.29	100.28	100.01	100.27
(ppm)								
Ba	503	407	670	1057	761	810	222	1682
Ce	66	90	86	96	104	57	46	140
Co	40	42	42	34	44	30	33	22
Cr	247	105	95	43	45	29	66	1
Cu	71	68	31	45	23	22	52	15
La	23	23	33	45	38	39	14	74
Nb	25	28	35	38	43	40	13	53
Ni	101	46	22	20	7	5	18	5
Rb	16	18	21	21	24	26	5	27
Sr	590	503	556	570	584	573	550	574
Th	2.81	ND	2.98	ND	3.41	4.18	3.55	4.23
U	0.650	ND	0.667	ND	0.809	1.06	0.758	0.943
Y	22	28	40	38	41	40	20	61
Zn	53	84	109	99	119	106	40	117
Zr	106	121	135	135	162	158	80	188

from reproduction of ($^{238}U/^{232}Th$) and ($^{230}Th/^{232}Th$) ratios of the A-THO standard (Williams et al. 1992) to within 2% (2σ) (Black 1994; Black et al. 1997).

The ^{226}Ra was measured using γ-spectrometry of its short-lived daughter ^{214}Pb at 352 MeV. Diffusion loss of the intermediate daughter ^{222}Rn from fine-grained material can affect ^{214}Pb activities; to overcome this all samples were sealed in airtight plastic containers with a capacity of 32 cm^3. Samples were counted on a Gamma-X high purity germanium coaxial photon detector, and to keep self-absorption differences negligible, the plastic containers were calibrated for a range of densities and masses (i.e. trachytes and basalts). Accuracy of the ^{226}Ra activities was assessed by running several samples that were known to be older than 8000 years. Sample KB121, a basalt from Emuruangogolak erupted 38,000 years ago gave a ($^{226}Ra/^{230}Th$) activity ratio = 1.04 ± 0.22, together with the Pleistocene rhyolitic obsidian from Iceland (A-THO) which gave ($^{226}Ra/^{230}Th$) activity ratio = 1.02 ± 0.12 (Williams et al. 1992).

Geochemical features

Rocks of the Upper Basalt Lavas range in composition from alkali olivine basalt to hawaiite, the transition being at MgO ~5 wt%. The two rock types are intercalated. All the rocks are mildly silica undersaturated (normative nepheline ≤ 3.4%). The most primitive basalt (KB119) has mg# [100 · mol MgO/(MgO + FeO)] = 62 and Cr and Ni abundances of 247 and 101 ppm, respectively. This almost certainly does not represent a primary magma and the suite has probably undergone gabbro fractionation deep within the crust (Macdonald 1994). This is consistent with major element variations in the sequence basalt-hawaiite, *viz*. increases in Na_2O, K_2O and P_2O_5 and decreases in Al_2O_3, MgO and CaO. Rocks with MgO ~5% show strong enrichment in FeO* (⩽15%) and TiO_2 (⩽4.2%) prompting Weaver (1977) to refer to them as high-Ti ferrobasalts.

Among the trace elements, fractionation from basalt to hawaiite involved increases in Ba, Ce, La, Nb, Rb, Th, U, Y and Zr, and decreases in Co, Cr, Ni and Sr. A feature of the trace element distribution is the scatter of concentrations at given MgO contents (e.g. Fig. 3), suggesting the existence of several magmatic lineages.

We have Sr-Nd-Pb isotopic data for three basalt-hawaiite samples (Table 2). The $^{87}Sr/^{86}Sr$ (0.703424–0.703439) and $^{143}Nd/^{144}Nd$ (0.512835–0.512855) show little variation within the basalts and hawaiites and are within the range of ocean island basalts (OIB). The range in Pb isotopic ratios is also small: $^{206}Pb/^{204}Pb$ = 19.289–19.548, $^{207}Pb/^{204}Pb$ = 15.584–

Table 1 b Major and trace element data for Emuruangogolak pantelleritic trachytes

Sample	KB245	KB258	KB61	KB150	KB141	KB143	KB90	KB91	KB93
Centre	Enab	Enab	Enab	Enab	Nak	Nak	Nak	Nak	Nak
Composition (Wt%)	PT	PT	PT	PT	PT	PT	PT	PT	PT
SiO_2	61.99	62.20	62.83	62.71	61.99	61.87	64.07	62.18	62.72
TiO_2	0.71	0.79	0.77	0.82	0.69	0.85	0.69	0.72	0.78
Al_2O_3	11.91	12.01	12.42	12.33	12.55	13.05	10.79	11.68	10.52
Fe_2O_3	10.11	10.31	9.82	10.19	9.88	9.58	10.40	10.62	11.54
MnO	0.39	0.33	0.40	0.37	0.34	0.34	0.31	0.36	0.42
MgO	0.31	0.21	0.26	0.17	0.36	0.37	0.17	0.37	0.15
CaO	1.76	1.59	1.58	1.68	1.51	1.90	0.88	1.84	1.14
Na_2O	6.77	6.17	6.65	6.12	6.67	6.20	6.87	6.52	7.44
K_2O	4.14	4.83	4.56	4.72	4.63	4.62	4.32	4.27	4.36
P_2O_5	0.02	0.09	0.06	0.09	0.08	0.12	0.03	0.05	0.05
LOI	1.22	0.67	0.66	0.15	0.70	0.50	1.20	1.05	0.68
Total	99.33	99.20	100.01	99.35	99.40	99.40	99.73	99.66	99.8
(ppm)									
Ba	352	506	442	512	505	133	253	339	238
Ce	194	221	198	233	175	375	265	203	261
Co	2	2	1	3	1	6	6	3	0
Cr	12	1	21	1	7	6	20	15	18
Cu	9	2	5	2	2	2	8	8	6
La	112	100	80	105	74	161	125	105	133
Nb	161	139	144	138	105	270	209	169	206
Ni	4	7	6	8	5	14	6	6	11
Rb	81	99	98	97	83	164	114	77	118
Sr	50	21	24	20	18	6	12	51	34
Th	9.11	9.98	9.38	9.78	6.99	5.74	13.57	9.16	13
U	2.00	2.11	2.03	2.40	1.96	1.32	3.52	2.41	ND
Y	121	101	97	99	78	170	140	117	131
Zn	261	201	214	206	187	355	308	254	323
Zr	709	541	533	531	413	1079	876	706	806

Table 1 b (continued)

Sample	KB144	KB97	KB60	KB86	KB96	KB47	KB79
Centre	Emur	Emur	Emur	Emur	Emur	Kapus	Kapus
Composition (Wt%)	PT	PT	PT	PT	PT	PT	PT
SiO_2	63.95	58.67	61.37	60.79	59.54	62.54	62.24
TiO_2	0.74	0.60	0.63	0.52	0.50	0.74	0.71
Al_2O_3	10.33	10.77	12.83	12.38	12.03	11.69	11.73
Fe_2O_3	11.07	10.86	10.15	10.67	10.68	10.53	10.25
MnO	0.39	0.36	0.36	0.37	0.35	0.38	0.35
MgO	0.12	0.10	0.20	0.17	0.10	0.17	0.19
CaO	0.94	1.15	1.57	1.44	0.96	1.07	1.64
Na_2O	6.70	7.04	6.84	7.87	8.98	7.10	6.96
K_2O	4.61	4.20	4.72	4.37	4.22	4.71	4.49
P_2O_5	0.07	0.04	0.07	0.06	0.07	0.06	0.04
LOI	0.45	0.93	0.91	1.13	0.70	0.78	1.33
Total	99.37	94.72	99.65	99.77	99.13	99.77	99.93
(ppm)							
Ba	849	512	243	132	138	172	192
Ce	116	249	168	271	288	187	184
Co	3	3	0	3	4	3	0
Cr	11	8	53	16	16	26	17
Cu	4	8	6	5	5	3	4
La	56	111	77	135	121	99	79
Nb	83	171	141	236	243	146	142
Ni	6	7	6	9	6	5	5
Rb	63	115	111	161	160	100	91
Sr	26	17	12	19	3	8	17
Th	7.21	6.84	13	17	15	11	11
U	2.11	2.01	ND	ND	ND	ND	ND
Y	61	117	87	140	145	96	96
Zn	151	266	209	296	295	240	228
Zr	308	645	530	916	934	542	527

Table 1 c Major and trace element data for Emuruangogolak comenditic trachytes

Number	KB244	KB99	KB80	KB89
Centre	Kapus	Kapus	Floor*	Floor*
Composition	CT	CT	CT	CT
(Wt%)				
SiO_2	62.99	63.42	62.68	61.89
TiO_2	0.81	0.73	0.84	0.93
Al_2O_3	15.02	15.17	14.75	15.48
Fe_2O_3	6.89	6.20	6.97	6.19
MnO	0.22	0.25	0.26	0.23
MgO	0.67	0.50	0.51	0.84
CaO	1.89	1.15	0.96	1.96
Na_2O	6.91	7.30	8.01	6.99
K_2O	4.01	4.55	4.95	4.05
P_2O_5	0.22	0.13	0.16	0.23
LOI	0.21	0.25	0.00	0.76
Total	99.84	99.65	100.09	99.55
(ppm)				
Ba	1576	1347	636	2264
Ce	141	145	121	130
Co	1	1	1	1
Cr	1	10	11	1
Cu	2	5	1	5
La	52	78	54	45
Nb	93	107	92	89
Ni	1	4	6	2
Rb	62	73	76	55
Sr	71	49	10	134
Th	8.01	7.18	6.94	7.19
U	1.98	1.50	1.22	1.42
Y	54	64	57	57
Zn	122	137	133	114
Zr	361	406	330	331

15.616 and $^{208}Pb/^{204}Pb$ = 39.122–39.367. The data form short linear arrays on Pb isotope correlation diagrams (Fig. 4a, b) and fall within the range of values observed for Northern Hemisphere OIB.

There is Th-U disequilibrium at 2σ confidence level in all our mafic samples, ranging from 27 to 42% Th excess (Fig. 5). The ($^{230}Th/^{232}Th$) ratios decay-corrected to the time of eruption ($^{230}Th/^{232}Th)_c$, are uniformly high (1.06–1.20), with a mean of 1.13 ± 0.06, corresponding to a mean calculated $[Th/U]_{source}$ ratio of 2.69 ± 0.11. Measured Th/U ratios are much higher (3.94–4.68). Low ($^{238}U/^{230}Th)_c$ ratios (0.59–0.72) indicate large relative U-Th fractionation. The ($^{234}U/^{238}U$) ratios are in secular equilibrium, within uncertainty. Four of the five samples are also characterised by excess (^{226}Ra) over (^{230}Th), by between 210 and 411%. This indicates that Ra-Th fractionation took place less than 8000 years before eruption.

The Upper Trachytes comprise both comenditic and pantelleritic varieties, with mol $(Na_2O + K_2O)/Al_2O_3$

Table 2 Sr-Nd-Pb isotopic ratios for Emuruangogolak basalts and trachytes. See text for uncertainties. (ND not determined)

Sample number	$^{206}Pb/^{204}Pb$	$^{207}Pb/^{204}Pb$	$^{208}Pb/^{204}Pb$	$^{87}Sr/^{86}Sr$	$^{143}Nd/^{144}Nd$
Upper Basalts					
KB46	19.480	15.613	39.306	0.703424	0.512855
KB82	19.531	15.612	39.343	0.703439	0.512835
KB145	19.465	15.609	39.278	0.703428	0.512847
Lower Basalts					
KB121	ND	ND	ND	0.703375	0.512863
Comenditic trachytes					
KB80	19.386	15.595	39.191	0.703629	0.512858
KB99	19.369	15.600	39.214	0.703737	0.512847
Pantelleritic trachytes					
KB97	19.548	15.616	39.367	0.704476	0.512852
KB144	19.289	15.599	39.170	0.704216	0.512842
KB150	19.298	15.584	39.122	0.704141	0.512862

Table 3 Whole rock U-Th-Ra isotope analyses for Emuruangogolak basalts and trachytes. *Brackets* denote activity ratios. *Subscript 'c'* refers to activity ratios decay-corrected to the time of eruption and *subscript 'm'* refers to activity ratios at time of measurement. ($^{226}Ra/^{230}Th$) ratios marked with an *asterisk* are decay-corrected to time of eruption. Uncertainties quoted are 2σ counting statistics

Sample number	Eruption age	$(^{238}U/^{232}Th)$	$(^{230}Th/^{232}Th)_m$	$(^{230}Th/^{232}Th)_c$	$(^{238}U/^{230}Th)_c$	$(^{234}U/^{238}U)$	$(^{226}Ra/^{230}Th)_m$
Upper Basalts							
KB145 (B)	(700–900)	0.695 ± 0.028	1.091 ± 0.041	1.094 ± 0.041	0.635 ± 0.035	0.998 ± 0.010	2.10 ± 0.21*
KB119 (B)	(700–900)	0.709 ± 0.026	1.195 ± 0.036	1.199 ± 0.036	0.591 ± 0.044	1.001 ± 0.010	4.11 ± 0.12*
KB59 (H)	(8000)	0.625 ± 0.023	1.028 ± 0.034	1.056 ± 0.034	0.592 ± 0.029	0.999 ± 0.016	1.06 ± 0.19
KB46 (H)	(250 ± 100)	0.826 ± 0.053	1.143 ± 0.040	1.144 ± 0.040	0.723 ± 0.047	1.000 ± 0.011	3.60 ± 0.15*
KB82 (H)	(700–900)	0.731 ± 0.025	1.141 ± 0.041	1.168 ± 0.041	0.626 ± 0.033	0.994 ± 0.014	2.51 ± 0.24*
Lower Basalts							
KB121 (H)	(38,000)	0.654 ± 0.021	1.002 ± 0.021	1.135 ± 0.021	0.576 ± 0.021	1.009 ± 0.011	1.04 ± 0.22
Comenditic trachytes							
KB80 (Floor)	(*c*.100)	0.539 ± 0.021	0.686 ± 0.026	0.686 ± 0.026	0.786 ± 0.024	0.999 ± 0.010	2.01 ± 0.11*
KB89 (Floor)	(3000)	0.605 ± 0.024	0.702 ± 0.021	0.705 ± 0.021	0.858 ± 0.022	0.995 ± 0.011	1.31 ± 0.13*
KB99 (Kapus)	(27,000)	0.641 ± 0.020	0.695 ± 0.022	0.717 ± 0.048	0.894 ± 0.031	1.011 ± 0.012	1.01 ± 0.12
KB244 (Kapus)	(27,000)	0.658 ± 0.012	0.781 ± 0.014	0.788 ± 0.014	0.835 ± 0.011	1.009 ± 0.011	1.10 ± 0.10
Pantelleritic trachytes							
KB144 (Emur)	(4000)	0.897 ± 0.021	0.847 ± 0.011	0.849 ± 0.011	1.057 ± 0.020	0.998 ± 0.014	1.03 ± 0.11
KB97 (Emur)	(16,000)	0.659 ± 0.034	0.853 ± 0.022	0.859 ± 0.022	0.767 ± 0.029	0.998 ± 0.009	0.99 ± 0.12
KB61 (Enab)	(38,000)	0.664 ± 0.018	0.845 ± 0.023	0.944 ± 0.053	0.703 ± 0.021	0.996 ± 0.010	0.99 ± 0.10
KB258 (Enab)	(38,000)	0.648 ± 0.031	0.864 ± 0.033	0.955 ± 0.033	0.679 ± 0.029	1.007 ± 0.011	1.04 ± 0.12
KB245 (Enab)	(38,000)	0.673 ± 0.021	0.850 ± 0.022	0.978 ± 0.022	0.688 ± 0.020	1.004 ± 0.009	1.05 ± 0.09
KB150 (Enab)	(38,000)	0.750 ± 0.025	0.959 ± 0.041	1.045 ± 0.041	0.718 ± 0.031	1.009 ± 0.011	1.08 ± 0.13
KB141 (Nak)	(4000)	0.860 ± 0.019	0.832 ± 0.014	0.831 ± 0.014	1.035 ± 0.018	1.000 ± 0.013	1.10 ± 0.10
KB143 (Nak)	(16,000)	0.704 ± 0.022	0.934 ± 0.024	0.971 ± 0.040	0.725 ± 0.026	0.996 ± 0.011	1.09 ± 0.11
KB90 (Nak)	(16,000)	0.795 ± 0.035	0.924 ± 0.037	0.948 ± 0.037	0.839 ± 0.039	0.995 ± 0.013	0.99 ± 0.13
KB91 (Nak)	(16,000)	0.807 ± 0.023	1.000 ± 0.022	1.037 ± 0.022	0.778 ± 0.021	0.999 ± 0.019	1.11 ± 0.14

values in the ranges 1.00–1.20 and 1.16–1.57, respectively. In keeping with their more peralkaline character, pantelleritic trachytes have, over approximately the same SiO_2 range, generally higher concentrations of FeO*, MnO, L (light) REE, Nb, Rb, Th, U, Y, Zn and Zr and lower abundances of Al_2O_3.

The comenditic trachytes have $^{87}Sr/^{86}Sr$ in the range 0.703629 to 0.703737, slightly more radiogenic than the basalts. The pantelleritic trachytes, on the other hand, have $^{87}Sr/^{86}Sr = 0.704141–0.704476$, significantly more radiogenic than the other rock types. The $^{143}Nd/^{144}Nd$ ratios in both groups of trachytes are similar to those in the basalts (Table 2). Pantelleritic trachytes from the northern flanks of the volcano and comenditic trachytes from the southern flanks have lower $^{206}Pb/^{204}Pb$ and $^{208}Pb/^{204}Pb$ than the basalts, whilst pantelleritic trachyte KB 97 has the highest $^{206}Pb/^{204}Pb$ and $^{208}Pb/^{204}Pb$ in our data set (Table 2).

The trachytes display variable Th-U disequilibria, ranging from 32% Th excess to 6% U excess at a 2σ confidence level (Fig. 5). The $(^{230}Th/^{232}Th)_c$ ratios range from 0.69 to 1.05 and there are distinct differences between the comenditic trachytes (0.686–0.788; mean 0.724 ± 0.045) and the pantelleritic trachytes (0.831–1.045; mean 0.942 ± 0.074). These ratios correspond to calculated $[Th/U]_{source}$ ratios of between 3.85 and 4.42 for the comenditic trachytes and 2.90 and 3.65 for the pantelleritic varieties and are clearly different from the basalt source ratios (2.69 ± 0.11). Measured Th/U ratios are much higher in the comenditic trachytes (4.05–5.69) but in the pantelleritic trachytes the Th/U ratios (3.40–4.73) are similar to those in the basalts (3.94–4.68). The $(^{238}U/^{230}Th)_c$ ratios range from 32% excess Th to 6% excess U (0.663–1.057). Two of the 14 trachytes [both comenditic, (KB80 and KB89)] have excess (^{226}Ra) over (^{230}Th) by between 201 and 131%, indicating recent (< 8000 years) Ra-Th fractionation.

Discussion

In Fig. 3 we flagged the possibility that the basalts and hawaiites represented several magmatic lineages. We now elaborate on that point, discussing both the mafic rocks and trachytes. A significant compositional variant among the hawaiites is KB59, which has notably low abundances of incompatible trace elements (ITE). The rock has a high Al_2O_3 content (20.86%), from which we may infer some plagioclase accumulation. However, a Rb/Zr ratio which is much lower (0.06) than in other basalts (0.15–0.16) indicates that the low ITE, especially LILE (large ion lithophile elements), abundances are not simply a function of dilution by plagioclase. Sample KB59 represents a magma type apparently rare in the Upper Basalts.

Among the other mafic lavas there are significant ranges in ITE ratios, e.g. Zr/Y 3.1–4.8, Rb/Ba 0.02–0.04, and K/La 199–346. The variations in these ratios are not due simply to fractional crystallisation; values for the hawaiites invariably lie within the basalt range. They

Table 4 U-Th-internal isochron data for whole rock and mineral separate analyses for three Emuruangogolak trachytes and one Paka trachyte. *Brackets* denote activity ratios. α_U and α_{Th} are distribution coefficients between alkali feldspar fractions and groundmass for U, Th and U/Th. Uncertainties quoted are all 2σ counting statistics

Sample number	$(^{238}U/^{232}Th)$	$(^{230}Th/^{232}Th)$	$(^{238}U/^{230}Th)$	$(^{234}U/^{238}U)$	Th (ppm)	U (ppm)	Th/U	α_U	α_{Th}	α_U/α_{Th}
KB61 (Enab)										
Whole rock	0.664 ± 0.018	0.845 ± 0.023	0.786 ± 0.019	0.996 ± 0.010	9.38	2.03	4.62			
Groundmass	0.615 ± 0.013	0.848 ± 0.013	0.725 ± 0.012	1.000 ± 0.011	10.62	2.13	4.99			
Alkali feldspar	0.610 ± 0.010	0.842 ± 0.012	0.725 ± 0.011	0.994 ± 0.014	0.51	0.10	5.03	0.047	0.048	0.979
Magnetic separate	0.854 ± 0.008	0.917 ± 0.007	0.951 ± 0.009	0.998 ± 0.010	0.58	0.16	3.59			
KB99 (Kapus)										
Whole rock	0.641 ± 0.020	0.695 ± 0.022	0.922 ± 0.021	1.011 ± 0.012	7.18	1.50	4.79			
Groundmass	0.667 ± 0.010	0.709 ± 0.010	0.941 ± 0.011	0.999 ± 0.016	8.27	1.81	4.57			
Alkali feldspar	0.611 ± 0.010	0.690 ± 0.009	0.886 ± 0.010	1.009 ± 0.011	0.53	0.11	5.02	0.061	0.064	0.953
Magnetic separate	0.840 ± 0.009	0.745 ± 0.008	1.128 ± 0.010	0.995 ± 0.012	0.55	0.15	3.65			
KB143 (Nak)										
Whole rock	0.704 ± 0.022	0.934 ± 0.024	0.754 ± 0.021	0.996 ± 0.011	5.74	1.32	4.35			
Groundmass	0.666 ± 0.013	0.935 ± 0.011	0.712 ± 0.012	0.999 ± 0.010	6.68	1.45	4.60			
Alkali feldspar	0.650 ± 0.011	0.930 ± 0.012	0.699 ± 0.012	0.995 ± 0.011	0.37	0.08	4.72	0.055	0.055	1.000
Magnetic separate	0.914 ± 0.009	0.964 ± 0.008	0.948 ± 0.008	1.011 ± 0.012	0.40	0.12	3.34			
Pak-3 (Paka Volcano)										
Whole rock	0.746 ± 0.014	0.806 ± 0.013	0.926 ± 0.011	1.004 ± 0.009	9.09	2.21	4.11			
Groundmass	0.682 ± 0.015	0.809 ± 0.019	0.843 ± 0.020	1.009 ± 0.011	12.90	2.87	4.49			
Alkali feldspar	0.692 ± 0.014	0.803 ± 0.016	0.890 ± 0.019	0.996 ± 0.011	0.492	0.111	4.43	0.039	0.038	1.026
Magnetic separate	0.942 ± 0.009	0.825 ± 0.009	1.142 ± 0.010	0.995 ± 0.013	0.911	0.280	3.25			

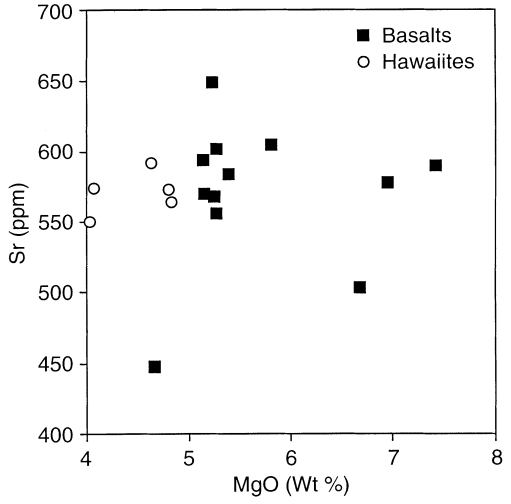

Fig. 3 MgO-Sr plot to show the scattered, multi-lineage, nature of basalts and hawaiites of the Upper Basalt Group. Data from this paper and Weaver (1977)

appear rather to be related to varying proportions of two components. One (represented by KB100, Table 1a) has high LILE/HFSE (high field strength elements) (e.g. Ba/Zr), LILE/LREE (Ba/La), LREE/HFSE (La/Nb) and low Zr/Nb; the other (KB94) has high Rb/Ba and K/La. The limited isotopic data suggest that the end-member with high Ba/Zr also has relatively high $^{87}Sr/^{86}Sr$ and $^{206}Pb/^{204}Pb$ and low $^{143}Nd/^{144}Nd$. Figure 6 shows the data array in terms of La/Nb versus Zr/Nb.

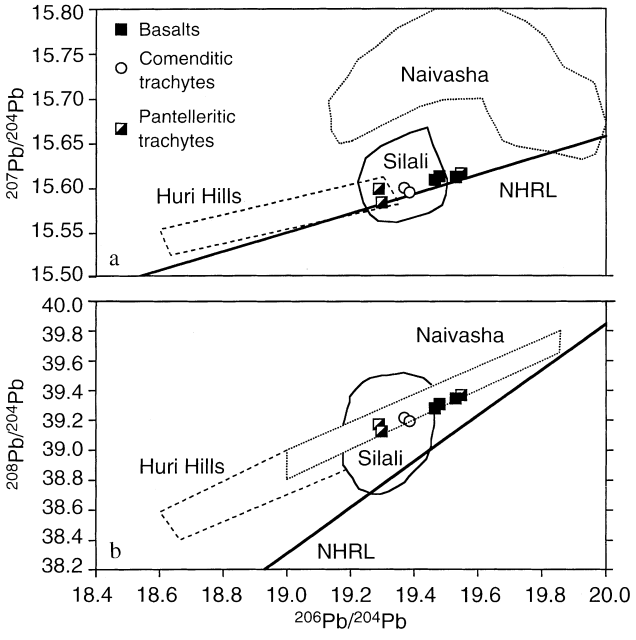

Fig. 4a, b $^{207}Pb/^{204}Pb$-$^{206}Pb/^{204}Pb$ and $^{208}Pb/^{204}Pb$-$^{206}Pb/^{204}Pb$ plots for Emuruangogolak basalts and trachytes. Fields for basalts from northern Kenya (Huri Hills, Norry et al. 1980), basalts and trachytes from Silali (Macdonald et al. 1995) and basalts and comendites from the Naivasha area (Davies and Macdonald 1987) are shown for comparison, together with the Northern Hemisphere Reference Line (*NHRL*)

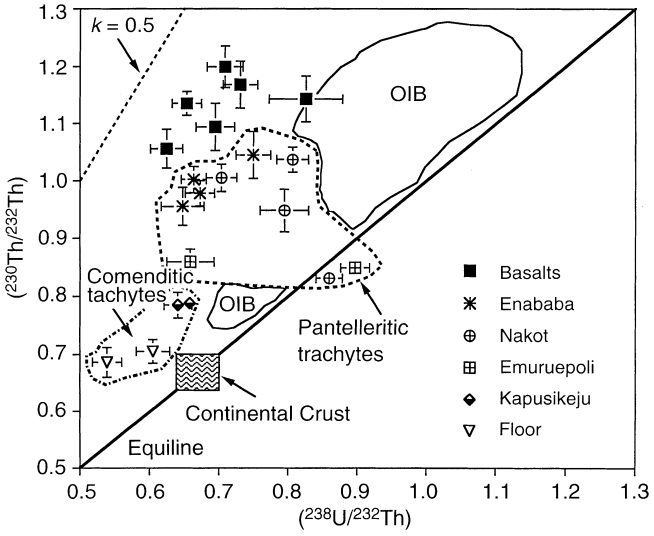

Fig. 5 ($^{238}U/^{232}Th$) versus ($^{230}Th/^{232}Th$) ratios. Fields for ocean island basalts (*OIB*) and continental crust are shown for reference (Condomines et al. 1988). Partial melting and radioactive decay trends are shown by the *arrows*. Value for $k = 50\%$ enrichment in ^{230}Th is shown by *dotted line*. Radioactive equilibrium at which (^{230}Th) = (^{238}U) is indicated by the *equilin*e. Uncertainties shown are at the 95% confidence level (2σ)

Linear correlations between pairs of ITE, particularly Zr and Nb (Fig. 7), were taken by Weaver (1977) as evidence that the Emuruangogolak trachytes were derived from basaltic magmas by fractional crystallisation. Isotopic data revealed a more complex petrogenesis (Norry et al. 1980). Whilst Nd isotopic ratios are broadly compatible with derivation of basalts and trachytes from a common source, the trachytes have higher $^{87}Sr/^{86}Sr$ than related basalts. An overall increase of $^{87}Sr/^{86}Sr$ with increasing Zr (used as a differentiation index) is consistent with evolution of the suite by com-

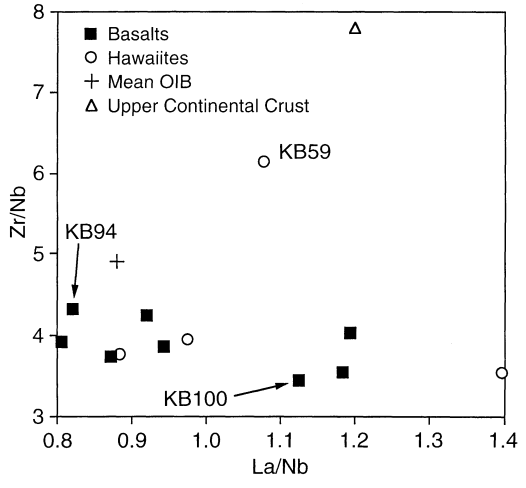

Fig. 6 Zr/Nb-La/Nb plot demonstrating the range of both ratios in the basalts and hawaiites. Mean OIB (from Fitton et al. 1991) and upper continental crust (Taylor and MacLennan 1985) compositions are shown for reference

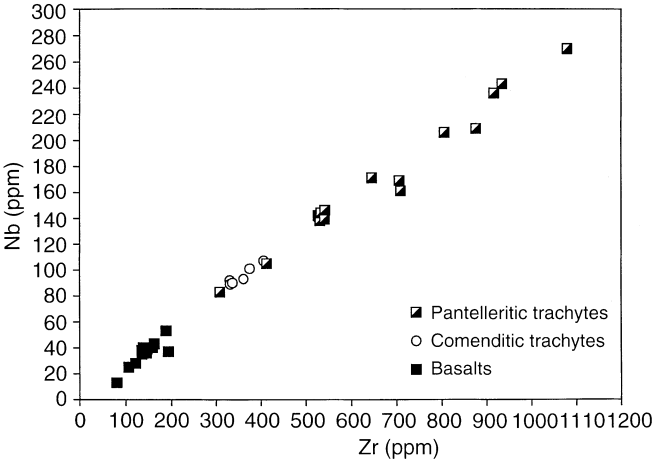

Fig. 7 Zr-Nb plot to show that superficially the basalts and trachytes apparently form a single magmatic lineage

bined assimilation-fractional crystallisation (AFC; Dunkley et al. 1993) of upper continental crust. In this model, the comenditic trachytes are intermediate between the basalts and pantelleritic trachytes.

This view of the relationship between basalts and trachytes is much too simplified, as we can show under two main headings.

1. The comenditic trachytes are not compositionally intermediate between basalts and pantelleritic trachytes. On a ($^{238}U/^{232}Th$)-($^{230}Th/^{232}Th$) plot, they occupy a quite different field to the other two groups. This is not a function of age difference because the data have been corrected to the eruption age. In addition, given the variations in $^{87}Sr/^{86}Sr$, both sets of data indicate that the basalts, comenditic trachytes and pantelleritic trachytes have been derived from different source rocks.
2. There are many magmatic lineages represented in the comenditic trachytes and pantelleritic trachytes. This is implicit in the isotopic variations (Figs. 4 and 5). It is also shown by the trace element data. The ratios Ce/Zr and Th/Nb will be relatively constant during alkali feldspar-dominated fractional crystallisation of peralkaline trachyte magmas, judging from the partition coefficient data of Mahood and Stimac (1990). Yet both ratios show significant ranges in the Emuruangogolak trachytes (Fig. 8).

We shall discuss the petrogenesis of the rocks in more detail elsewhere. Here, we stress the point that the trachytes, like the basalts, represent a (large) number of liquid lines of descent, which resulted from generation in variable source rocks and/or different evolutionary histories.

Four important points can be made concerning the compositional variations in space and time:-

1. Essentially coeval basalts and trachytes were not intimately related genetically, but have been derived from isotopically different sources (Figs. 4, 5, Table 2).

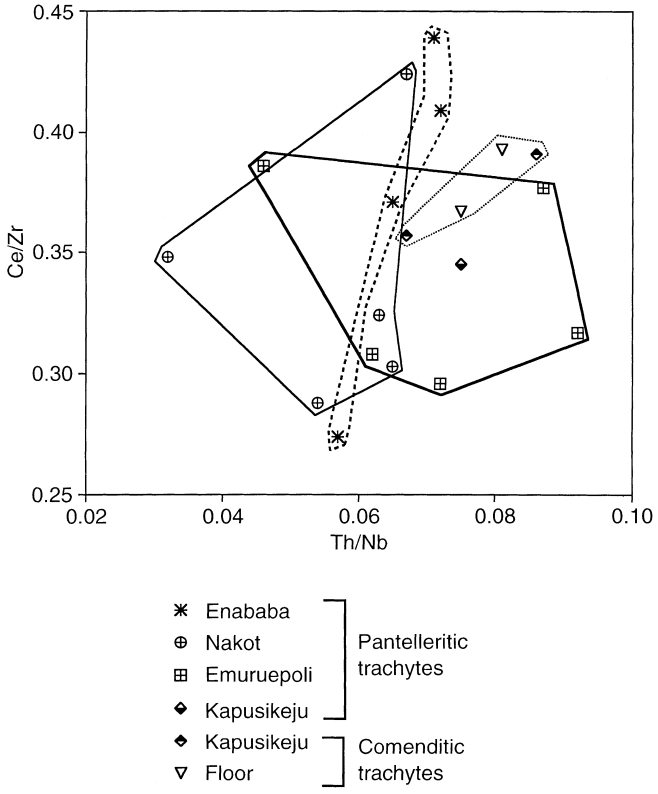

Fig. 8 Ce/Zr-Th/Nb plot to show the multi-lineage nature of the trachytes, even within stratigraphic groups. Neither ratio should be changed significantly by closed system fractional crystallisation of alkali feldspar-dominated assemblages

2. Basalts of the same age can be compositionally distinct. For example, three mafic lavas erupted 900–700 years ago (KB82, KB119 and KB145) are isotopically slightly different (Tables 2 and 3; Fig. 5) and have different ITE ratios, e.g. K/La ratios of 260, 346 and 277, respectively.
3. There is considerable compositional variation within the Upper Trachyte lavas which is not due simply to either fractional crystallisation or AFC. For example both Emuruepoli and Nakot groups contain lavas which are U-enriched and U-depleted, i.e. plotting on both sides of the equiline in Fig. 5, indicating different source magmas or melting conditions. In addition, both pantelleritic trachytes and comenditic trachytes have been erupted from the Kapesikeju centre.
4. There are also significant differences between the groups. Pantelleritic trachytes from Kapesikeju, for example, show no overlap with similar rocks from Nakot on the Ce/Zr-Th/Nb plot (Fig. 8) and lavas from Emuruepoli and Enababa, eruptions of which overlapped in time (Fig. 2), have different ($^{230}Th/^{232}Th$) ratios.

It appears, therefore, that over periods as short as 5000 years, the eruptive span of the Enababa group, compositionally diverse, and genetically only broadly related, magmas were erupted from the same plumbing system(s). Inter-group variations, even when the groups overlapped in time, suggest that there have been several such plumbing systems at Emuruangogolak.

Preservation of the isotopic and trace element differences between the magmas indicates that they have not been homogenised by mixing in a large-scale magma chamber of the type envisaged for the nothern Kenya caldera volcanoes by Macdonald (1987). We infer, therefore, that eruptive activity at Emuruangogolak is fed mainly by dykes. This is in accord with geological, geomorphological and geophysical evidence, discussed earlier, for zones of multiple dyke injection close to the surface. An implication of this is that if the trachytes are stored in large reservoirs, e.g. cupolas or sill-like bodies, these reservoirs must be capable of collapsing, to allow new batches of magma to pass through without significant homogenisation with previous magma batches.

We have inferred that over the past 38 ka a very large number of magma batches, only broadly related genetically, have passed through the high-level plumbing system at Emuruangogolak.

Timescales of magma production

Earlier work (Weaver 1977; Dunkley et al. 1993) established that the mafic lavas of Emuruangogolak are high-Fe-Ti basalts of transitional affinity, the Upper Basalts being nepheline-normative. Basalts of this type are common in the Quaternary sequences of the rift floor and are also important constituents of the lava fields of the western and eastern flanks. The fact that they straddle the critical plane of silica-undersaturation suggests that they fractionated at pressures equivalent to the base of the crust. Macdonald (1994) suggested that the parental magmas were delayed at Moho depths and underwent variable degrees of fractionation along olivine-plagioclase-augite cotectics. The nepheline-normative character of the Upper Basalts points to a limited fractionation history within the crust, as do the Sr isotopic ratios ($^{87}Sr/^{86}Sr < 0.70344$).

The Th-U disequilibria data suggest that the transport of the basalts from the source zone to the surface has been relatively rapid, as some display ($^{226}Ra/^{230}Th$) ratios >1 (Table 3). Further quantification of the time of formation of the mafic rocks is prohibited due to variations in $(^{226}Ra)_0/Ba$ ratios ($2.5–6.7 \times 10^{-3}$ dpm/mg) (Tables 1 and 3). Two of the youngest comenditic trachyte magmas (KB 80 and KB89 erupted 100 and 3000 years ago, respectively) also show ($^{226}Ra/^{230}Th$) activity ratios >1 indicating recent (<8000 years) fractionation of Ra from Th.

Magmatic residence times

U-Th internal isochrons

The ^{238}U-^{230}Th internal isochron method is based on the restoration with time of equilibrium between the prog-

eny ^{230}Th and parent ^{238}U after initial relative U:Th fractionation during magma evolution (e.g. Condomines et al. 1988; Gill and Condomines 1992). The isochron approach applies to cogenetic minerals that have different initial degrees of U-Th fractionation. The isochron is described by the equation (Allègre 1968):

$$\left(\frac{^{230}\mathrm{Th}}{^{232}\mathrm{Th}}\right)_t = \left(\frac{^{230}\mathrm{Th}}{^{232}\mathrm{Th}}\right)_0 e^{-\lambda t} + \left(\frac{^{238}\mathrm{U}}{^{232}\mathrm{Th}}\right)_t \left(1 - e^{-\lambda t}\right) \quad (1)$$

^{232}Th is used as a reference radionuclide for normalisation purposes. The half-life of ^{230}Th is taken to be 75.38 ka, which implies that secular equilibrium would be approached after some 350 ka.

Three trachytes were selected for internal U-Th isochron analyses to try to quantify the post-phenocryst crystallisation residence time of the magmas beneath Emuruangogolak (Table 4). The three samples (all from the Upper Trachyte lavas) can be seen in Fig. 9a–c, together with an internal isochron from a post-caldera trachyte, from the Paka volcano, for comparison (Fig. 9d). They were selected to include both pantelleritic (KB61 and KB143), and comenditic (KB99) trachyte varieties. These are the first reported trachyte internal isochrons from the Kenya Rift Valley. Table 4 also shows the internal isochron data together with the mineral fraction-groundmass data. The isochrons show large displacements to the right of the equiline by the magnetic fractions. Condomines et al. (1982) have shown that partitioning of U and Th into a magnetic fraction is the most important for U-Th dating; our data confirm this. The alkali feldspar fractions have $\alpha_U/\alpha_{Th} = 0.95$–$1.03$ and are similar to the plagioclase phenocryst value reported in Condomines et al. (1982).

Interpretation

The three isochrons give U-Th crystallisation ages between 14,000 and 40,000 years (Fig. 9a, b and c), which are comparable to the alkali feldspar ^{40}Ar/^{39}Ar ages reported in Dunkley et al. (1993) (Table 5) for the same samples. The post-crystallisation residence time, i.e. the difference between the U-Th crystallisation age and the ^{40}Ar/^{39}Ar age of the trachyte magmas, is thus negligible, within the analytical uncertainties of the two techniques.

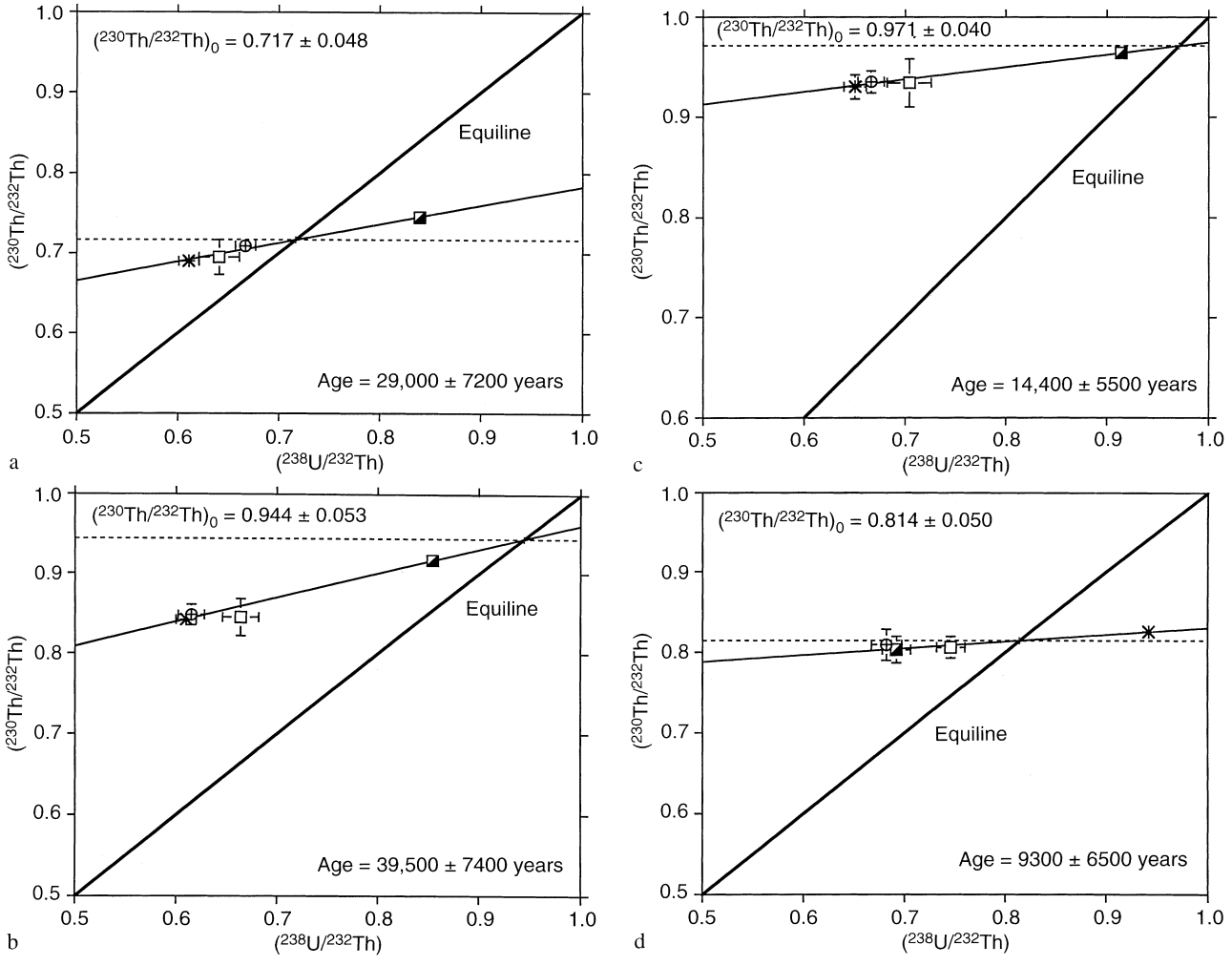

Fig. 9a–d Internal isochrons for samples (a) KB99 (Kapusikeju group), (b) KB61 (Enababa group), (c) KB143 (Nakot group) and (d) Paka-3 (Paka volcano). (*Open square* whole rock, *hash* alkali feldspar, *crossed circle* glass, *diagonally filled square* magnetic separate)

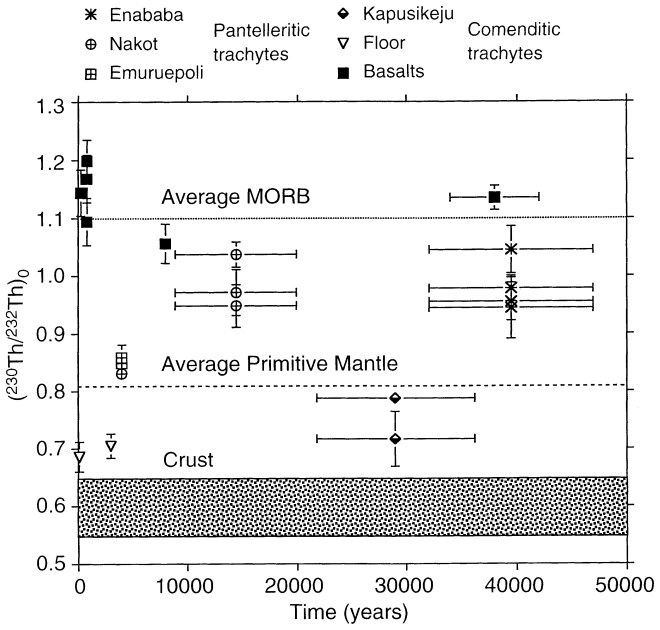

Fig. 10 Variation of initial $(^{230}Th/^{232}Th)_0$ as a function of time for Emuruangogolak basalts and trachytes. See text for explanation

Table 5 Comparison of U-Th and $^{40}Ar/^{39}Ar$ ages for the Upper Trachyte lavas for Emuruangogolak and Paka. Uncertainties quoted for the U-Th isochron age are 2σ counting statistics. $^{40}Ar/^{39}Ar$ ages from Dunkley et al. (1993); uncertainties quoted are 2σ

Sample	U-Th isochron age (years)	Single crystal, laser fusion $^{40}Ar/^{39}Ar$ ages (years)
Emuruangogolak		
KB 61 (Enab)	$39{,}500^{+7800}_{-7200}$	38,000 ± 3000
KB 99 (Kapus)	$29{,}000^{+7500}_{-7000}$	27,000 ± 5000
KB 143 (Nak)	$14{,}400^{+5700}_{-5400}$	16,000 ± 5000
Paka		
Pak-3	9300^{+6700}_{-6300}	11,000 ± 3000

A similar situation may also hold at Paka (Fig. 9d), where the analysed trachyte gives an identical U-Th age to its feldspar $^{40}Ar/^{39}Ar$ age, indicating that the relationship may be common to the northern centres.

Crystallisation ages of various volcanic suites have been recorded (e.g. Black et al. 1997; Black et al. in press; Bourdon et al. 1994; Condomines et al. 1982a, b; Deniel et al. 1992; Fukuoka 1974; Fukuoka and Kigoshi 1974; Pyle et al. 1988; Reagan et al. 1992; Sampson et al. 1984; Schaefer et al. 1993; Volpe and Hammond 1991; Volpe 1992). However, the U-Th criteria for absolute age determination of young volcanic rocks, particularly those displaying initial isotopic homogeneity, may not always be satisfied (Capaldi and Pece 1981; Hêmond and Condomines 1985). Clear evidence of crystallisation ages and their relationships to eruption ages of magmas have been reported only rarely (Black et al. 1997; Black et al. in press; Bourdon et al. 1994; Condomines et al. 1982a; Condomines 1997; Deniel et al. 1992; Pyle et al. 1988; Reagan et al. 1992; Sampson et al. 1984; Schaefer et al. 1993; Volpe and Hammond 1991; Volpe 1992), and these indicate that relatively short residence times (0–30 ka) are likely, although longer residence times of 10^4–10^5 years have been recorded from volcanic complexes on active continental margins, e.g. Western USA (Mt. Mazama, Inyo domes and Mono Craters). Some of these examples may, however, involve reworked older crystals (e.g. Pyle et al. 1988).

$(^{230}Th/^{232}Th)_0$ initial ratio variations

The ^{238}U-^{230}Th disequilibria technique can be used to determine the main steps in magmatic evolution, as well as to date magmatic events (Condomines et al. 1988). In particular, the variation of $(^{230}Th/^{232}Th)_0$ is useful for interpreting the evolution of a magmatic system. When magmas are extracted from the same magmatic reservoir evolving as a closed system, on a long timescale relative to the half-life of ^{230}Th (half-life = 75,380 years), their initial $(^{230}Th/^{232}Th)_0$ ratios vary linearly when plotted against $e^{\lambda t}$, providing that isotopic homogenization occurs within the magma.

The $(^{230}Th/^{232}Th)_0$ of the Emuruangogolak magma when phenocryst crystallisation began can be deduced from Fig. 9a–c. The ratios are plotted as a function of time ($e^{\lambda t}$) in Fig. 10. Basalts and samples from the same trachytic group, were age-corrected back to the isochron age obtained for that group, assuming a similar crystallisation age for all samples within that group. This situation is not ideal as we do not know if all the groups crystallised at the same time, but relative variations in within-group $(^{230}Th/^{232}Th)_0$ ratios are small. It is clear from Fig. 10 that Emuruangogolak has erupted magmas with a very large range in initial $(^{230}Th/^{232}Th)_0$ ratios, from basalts with high (≥1.1) ratios to comenditic trachytes with low (≤0.8) ratios over a very short period of time (< 40 ka). This, together with Sr-Nd-Pb data, provides further evidence that the system is very open and that not enough time has elapsed to produce the low $(^{230}Th/^{232}Th)$ ratios of the trachytes from the basalts through closed system processes.

Concluding remarks

1. Young trachytes of the Emuruangogolak volcano are divisible into comenditic and pantelleritic varieties, which have isotopic characteristics different to each other and to associated basalts. The two types of trachyte cannot have been derived from the same sources, or formed by the same genetic mechanism.
2. The basalts, comenditic trachytes and pantelleritic trachytes each comprise several magmatic lineages. Several, compositionally different magmas have been erupted over the past 38 ka, sometimes as parts of the same stratigraphic group.

3. Young basalts exhibit significant excess (^{230}Th) over (^{238}U), indicating a fractionation event at less than 0.3 Ma. Four of five samples analysed also have excess (^{226}Ra) over (^{230}Th), implying Ra-Th fractionation < 8 ka.
4. U-series internal isochrons for 3 trachytes give phenocryst crystallisation ages comparable to eruption ages, suggesting that crustal residence times were very short.
5. The Emuruangogolak plumbing system is markedly open; a large number of genetically unrelated basalts and trachytes have been processed through it without significant homogenization.

Acknowledgements We thank Michel Condomines and Dave Pyle for very helpful reviews which greatly improved the manuscript. Lancaster work in Kenya is supported by Natural Environment Research Council Lewehulme Trust and The Nuffield Foundation.

References

Allègre CJ (1968) ^{230}Th dating of volcanic rocks: a comment. Earth Planet Sci Lett 90: 243–263

Black S (1994) U-Th disequilibria systematics of the Olkaria complex Gregory Rift Valley, Kenya, (unpublished). PhD thesis, Univ Lancaster

Black S, Macdonald R, Kelly M (1997) Crustal origin for peralkaline rhyolites from Kenya: evidence from U-series disequilibria and Th-isotopes. J Petrol 38, 2: 277–297

Black S, Macdonald R, DeVivo B, Kilburn CRJ, Rolandi G (1998) U-series disequilibria in young (A.D. 1944) Vesuvius rocks: preliminary implications for magma residence times and volatile addition. J Volcanol Geothermal Res (in press)

Bourdon B, Zindler A, Worner G (1994) Evolution of the Laacher See magma chamber: evidence from SIMS and TIMS measurements of U-Th disequilibria in minerals and glasses. Earth Planet Sci Lett 126: 75–90

Capaldi G, Pece R (1981) On the reliability of the ^{230}Th-^{238}U dating method applied to young volcanic rocks. J. Volcanol Geothermal Res 11: 367–372

Condomines M (1997) Dating recent volcanic rocks through ^{230}Th-^{238}U disequilibrium in accessory minerals: example of the Puy de Dôme (French Massif Central). Geology 25: 375–378

Condomines M, Morand P, Camus G, Duthou L (1982a) Chronological and geochemical study of lavas from the Chaine des Puys, Massif Central, France: evidence for crustal contamination. Contrib Mineral Petrol 81: 296–303

Condomines M, Bouchez R, Ma JL, Tanguy JC, Amosse J, Piboule M (1982b) Short-lived radioactive disequilibria and magma dynamics in Etna volcano. Geochim Cosmochim Acta 46: 1397–1496

Condomines M, Hêmond C, Allègre CJ (1988) U-Th-Ra radioactive disequilibria and magmatic processes. Earth Planet Sci Lett 90: 243–263

Davies GR, Macdonald R (1987) Crustal influences in the petrogenesis of the Naivasha basalt-rhyolite complex; combined trace element and Sr-Nd-Pb isotope constraints. J Petrol 28: 1009–1031

Deniel G, Kieffer G, Lecointre J (1992) New ^{230}Th-^{238}U and ^{14}C determinations from Piton des Neiges volcano, Reunion – a revised chronology for the Differentiated Series. J Volcanol Geothermal Res 51: 253–267

Dunkley PN, Smith M, Allen DJ, Darling WG (1993) The geothermal activity and geology of the northern sector of the Kenya Rift Valley. Br Geol Surv Res Rep SC/93/1

Fitton JG, Jame D, Leeman W (1991) Basic magmatism associated with late Cenozoic extension in the Western United States: compositional variations in space and time. J Geophys Res 96: 13693–13711

Fukuoka T (1974) Ionium dating of acidic volcanic rocks. Geochem J 8: 109–116

Fukuoka T, Kigoshi K (1974) Discordant Io-ages and the U, Th distribution between zircon and host. Geochem J 8: 117–122

Gill JB, Condomines M (1992) Short-lived radioactivity and magma genesis. Science 257: 1368–1376

Hêmond C, Condomines M (1985) On the reliability of the ^{230}Th-^{238}U dating method applied to young volcanic rocks – discussion. J Volcanol Geothermal Res 26: 365–368

Hillaire-Marcel C, Carro O, Casanova J (1986) ^{14}C and Th/U dating of Pleistocene and Holocene stromatolites from East African paleolakes. Quat Res 25: 312–329

Macdonald R (1987) Quaternary peralkaline silicic rocks and caldera volcanoes in Kenya. In: Fitton JG, Upton BGJ (eds) Alkaline igneous rocks. Geol Soc London Spec Publ 30, pp 313–333

Macdonald R (1994) Petrological evidence regarding the evolution of the Kenya Rift Valley. Tectonophysics 236: 373–390

Macdonald R, Davies GR, Upton BJG, Dunkley PN, Smith M, Leat PT (1995) Petrogenesis of Silali volcano, Gregory Rift, Kenya. J Geol Soc London 152: 703–720

Mahood G (1984) Pyroclastic rocks and calderas associated with strongly peralkaline magmatism. J Geophys Res 89, NB10: 8540–8552

Mahood G, Stimac JA (1990) Trace-element partitioning in pantellerites and trachytes. Geochim Cosmochim Acta 54: 2257–2276

Norry MJ, Truckle PH, Lippard SJ, Hawkesworth CJ, Weaver SD, Marriner GF (1980) Isotopic and trace element evidence from lavas, bearing on mantle heterogeneity beneath Kenya. Philos Trans R Soc London A297: 259–271

Pyle DM, Ivanovich M, Sparks RSJ (1988) Magma-cumulate mixing identified by U-Th disequilibrium dating. Nature 331: 157–159

Reagan MK, Volpe AM, Cashman KV (1992) ^{238}U- and ^{232}Th-series chronology of phonolite fractionation at Mount Erebus, Antarctica. Geochim Cosmochim Acta 56: 1401–1407

Sampson DE, Williams RW, Robin M, Gill JB (1984) The age of rhyolitic magma at eruption, Inyo volcanic chain, eastern California. EOS Trans Am Geophys Union 65: 1129

Schaefer SJ, Sturchio NC, Murrell MT, Williams SN (1993) Internal ^{238}U-series systematics of pumice from the November 13, 1985, eruption of Nevado del Ruiz, Columbia. Geochim Cosmochim Acta 57: 1215–1219

Skilling IP (1993) Incremental caldera collapse of Suswa volcano, Gregory Rift Valley, Kenya. J Geol Soc London 150: 885–896

Skinner NJ, Iles W, Brock A (1975) The recent secular variation of declination and inclination in Kenya. Earth Planet Sci Lett 25: 338–346

Smith M, Dunkley PN, Deino A, Williams AAJ, McCall GJH (1995) Geochronology, stratigraphy and structural evolution of Silali volcano, Gregory Rift Valley. J Geol Soc London 152: 297–310

Swain CJ (1976) Some gravity results from the northern Gregory Rift. In: Pilger A, Rossler A (eds) Afar between continental and oceanic rifting. Schweizerbart'sche, Stuttgart, pp 120–125

Swain CJ (1992) The Kenya Rift axial gravity high: a reinterpretation. Tectonophysics 204: 59–70

Taylor SR, McLennan SM (1985) The continental crust; its composition and evolution. Blackwell, Oxford

Volpe AM (1992) ^{238}U-^{230}Th-^{226}Ra disequilibrium in young Mt. Shasta andesites and dacites. J Volcanol Geothermal Res 53: 227–238

Volpe AM, Hammond PE (1991) ^{238}U-^{230}Th-^{226}Ra disequilibrium in young Mount St. Helens volcanics: time constraint for magma formation and crystallisation. Earth Planet Sci Lett 107: 475–486

Weaver SD (1977) The Quaternary caldera volcano Emuruangogolak, Kenya Rift, and the petrology of a bimodal ferrobasalt-pantelleritic trachyte association. Bull Volcanol 40: 209–230

Widom E, Schmincke H-U, Gill JB (1992) Processes and timescales in the evolution of a chemically zoned trachyte: Foga A, Sao Miguel, Azores. Contrib Mineral Petrol 111: 311–328

Williams LAJ, Macdonald R, Chapman GR (1984) Late Quaternary caldera volcanoes of the Kenya Rift. J Geophys Res 89 B10: 8553–8570

Williams RW, Collerson KD, Gill JB, Deniel C (1992) High Th/U ratios in subcontinental lithospheric mantle: mass spectrometric measurements of Th isotopes in Gaussberg lamproites. Earth Planet Sci Lett 111: 257–268

Williamson JH (1968) Least-squares fitting of a straight line. J Phys 46: 1845–1847